# Nanoscale

Accepted Manuscript


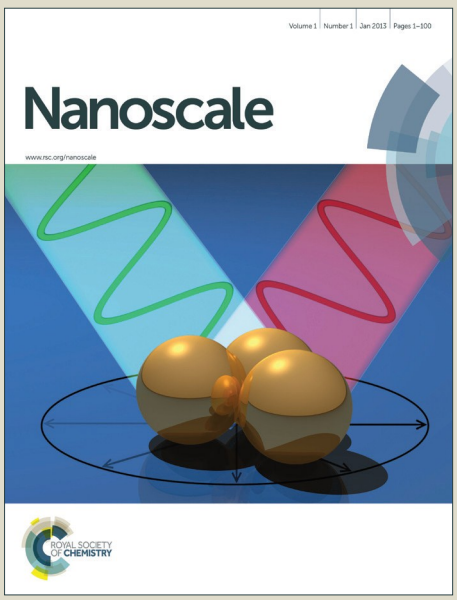





ROYAL SOCIETY OF CHEMISTRY

www.rsc.org/nanoscale

Nanoscale

COMMUNICATION

# A fluorometric microarray with ZnO substrate-enhanced fluorescence and suppressed "coffee-ring" effects for fluorescence immunoassays

Shuying Li, Minmin Dong, Rui Li, Liyan Zhang, Yuchun Qiao, Yao Jiang, Wei Qi, and Hua Wang *

Received 00th January 20xx,
Accepted 00th January 20xx

DOI: 10.1039/x0xx00000x

www.rsc.org/chemcomm

**Glass slide was first patterned with hydrophobic hexadecyltrimethoxysilane (HDS) and then microspotted with hydrophilic ZnO nanoparticles in aminopropyltriethoxysilane (APS) matrix. The resulted HDS-ZnO-APS microarray could present the capability of suppressing the formidable "coffee-ring" effects through its hydrophobic pattern so as to allow for the fabrication of ZnO-APS testing microspots with highly dense and uniform distribution. Lotus-like "self-cleaning" function could also be expected to effectively curb the crossing contamination of the multiple sample droplets. More importantly, the introduction of ZnO nanoparticles could endow the testing microspots with the substrate-enhanced fluorescence leading to the signal-amplication microarray fluorometry. The practical application of the deveoped HDS-ZnO-APS microarray was investigated by the sandwiched fluorometric immunoassays of human IgG, showing a linear detection range from 0.010 to 10.0 ng mL$^{-1}$. Such a throughput-improved fluorometric microarray could be tailored for probing multiple biomarkers in the complicated media like serum or blood.**

Fluorometric microarray technologies have sparkled increasing interests of the practical research applications for the analysis of multiple samples.[1-6] For example, antibody microarray has been widely developed by coupling with the fluorescent signal amplification for the fluorometric analysis of massive biological targets.[6] It is widely recognized that the detection throughput and analysis sensitivity can play vital roles in the analysis performances of microarrays. However, the detection throughput can be generally limited by the distribution density of testing microspots on the microarrays and the risk of formidable fouling or crossing contamination of multiple samples. Accordingly, many efforts have been devoted to the improvement of the detection throughput of the microarrays or microchips.[7-11] For example, Roy and co-workers etched the fluorocarbon layer by photolithographic way to build dense microspots toward a high throughput microchip for the microRNA detections.[8] Levkin *et al*. fabricated the hydrophobic barriers for the hydrophilic testing areas by the UV-initiated masking technique to prevent the cross-contamination of the multiple samples between adjacent microspots for genome-wide cell screens.[9] On the other hand, the detection sensitivity of microarray can mostly depend on the signal amplification of the responses to targets. In recent decades, many signal enhancement protocols have been developed to realize the highly sensitive microarray detections, most known as the enzyme-triggered chemiluminescence,[12] rolling-circle amplification,[13] tyramide-based signal amplification,[14] *photoelectrochemical or electrochemiluminescence methods*,[15-17] and immune-gold silver staining.[18] Although various microarray fabrications and signal amplification strategies have been developed, they might suffer from some disadvantages such as the complicated fabrication procedures, tedious signal amplification steps, time-consuming operations, and serious background interferences.

Recent years have witnessed the wide applications of nanomaterials of metals (i.e., silver nanoparticles) and metal oxides (i.e., ZnO nanomaterials) for improving the fluorometric performances especially the signal enhancement of fluorometric analysis.[19-23] For example, Alam *et al*. utilized silver nanoparticles to enhance the fluorescence of terbium complexes for probing the catecholamine.[20] Punnoose's group employed ZnO nanoparticles to achieve the fluorescence enhancement of dye via the energy transfer.[21] Such a straightforward fluorescence-enhancement protocol can circumvent the disadvantages of most of the complicated signal amplification strategies aforementioned. Unfortunately, we initially tried to employ ZnO nanoparticles to fabricate the testing microspots of microarray, the ring-staining or donut-like testing spots were observed with very poor distribution density and uniformity, as also reported for other kinds of nanoparticles elsewhere.[24-26] Herein, ZnO nanoparticle

Shandong Province Key Laboratory of Life-Organic Analysis, College of Chemistry and Chemical Engineering, Qufu Normal University, Qufu City, Shandong Province 273165, P. R. China. E-mail address: huawangqfnu@126.com; Tel: +86 5374456306; Fax: +86 5374456306; Web: http://wang.qfnu.edu.cn.

Electronic Supplementary Information (ESI) available.
See DOI: 10.1039/x0xx00000x

Nanoscale

COMMUNICATION

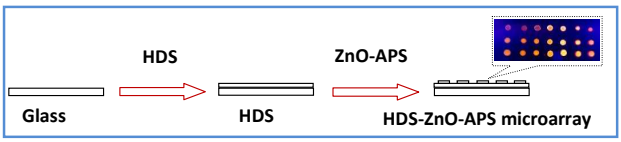


**Scheme 1** Schematic illustration of the fabrication procedure of HDS-ZnO-APS microarray created first with the hydrophobic HDS and then with the hydrophilic ZnO-APS microspots.

droplets on the microarray would be carried to their edges to form ring-like deposits along the perimeter after the solvent evaporation, most known as the "coffee-ring" effects.[27] Historically, the "coffee-ring" effects were improved typically by introducing surfactants or polymers to optimize the spotting solutions for the microarray fabrications.[28, 29] Very recently, Stauber *et al.*[30] theoretically demonstrated that the hydrophobic surfaces could influence the evaporation of droplets both in the constant contact radius and contact angle modes, which is expected to suppress the "coffee-ring" effects on the hydrophobic substrates.

Inspired by these pioneering works above, in the present work, glass slides were first patterned with hydrophobic hexadecyltrimethoxysilane (HDS) and then microspotted with hydrophilic ZnO nanoparticles in aminopropyltriethoxysilane (APS) matrix (ZnO-APS), as illustrated in **Scheme 1**, resulting in fluorometric microarray with ZnO substrate-enhanced fluorescence. Herein, the HDS-patterned hydrophobic surfaces could, on the one hand, facilitate the amine-derivatized ZnO-APS microspots to be densely and uniformly distributed on the microarray with the "coffee-ring" effects largely suppressed. On the other hand, they could functionalize lotus-like "self-cleaning" to effectively curb the fouling or cross-contamination of the samples between the adjacent hydrophilic ZnO-APS microspots. Also, the HDS patterns are transparent enough to be tailored for the optical observations or measurements. More importantly, the resulting fluorometric HDS-ZnO-APS microarray could achieve the ZnO substrate-enhanced fluorescence toward the highly-sensitive fluorometric immunoassays as shown in the microarray photograph (inset).

The "coffee-ring" effects-against performances of the so prepared HDS-ZnO-APS microarray were investigated by comparing with those deposited on the normal glass slides, taking the APS microspots and the blank (none) as the controls (**Fig. 1**). As characterized by the fluorescent microscope images both in light and dark fields (**Fig. 1a**, the first column), ZnO-APS microspots could be uniformly distributed on the HDS-patterned substrates with no significant "coffee-ring" effects. In contrast, the ZnO-APS microspots constructed on the normal glass slides without HDS patterns showed obviously extended edges and ring-staining shapes of solid spots (**Fig. 1b**, the first column). Additionally, ZnO nanoparticles in the APS matrix were found to enable the testing microspots formed beyond the surfaces of hydrophobic substrate so as to avoid any in-between fouling or crossing contamination of sample droplets, as comparably shown in the photographs of sample tests (**Fig. 1**). Furthermore, the performances of the so developed ZnO-APS microarray against the crossing contamination of samples were comparably explored by the sample tests using red rhodamine B (RB) as a visible sample model (**Fig. 1**, the third column). The photographic results illustrated that RB droplets could be uniformly diffused on the HDS-patterned hydrophobic slides with ideally shrunk shapes (**Fig. 1a**, the third column). In contrast, they exhibited the serious "coffee-ring" stains on the normal glass slides without HDS patterns (**Fig. 1b**, the third column). Of note, the HDS-patterned hydrophobic substrates might provide a self-cleaning interface between the testing microspots so as to prevent the possible nonspecific adsorption or background interference and the crossing contamination from the multiple

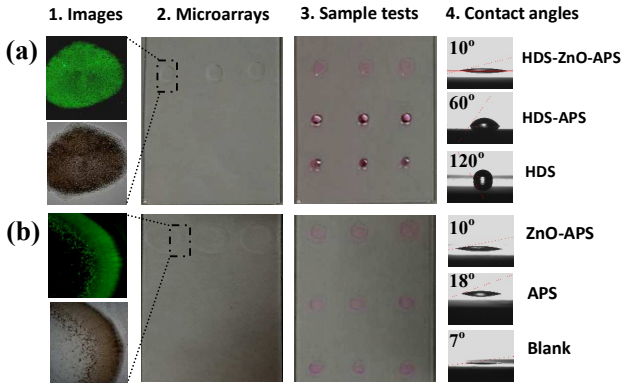


**Fig. 1** The comparison of "coffee-ring" effects-suppressed performances between (**a**) HDS-patterned, and (**b**) normal glass microarray slides modified separately with none (blank), APS, and ZnO-APS microspots (from bottom to top, each line for tri-replicated microspots) using 5.0 % HDS and 1.0 % APS or ZnO-APS, characterized by fluorescent microscope images of light and dark fields (first column), photographs (second and third column), and contact angles (forth column) measured using 1.0 μL fluorescent RB.

samples on the microarray. As manifested by the data of contact angles, the so formed ZnO-APS microspots on HDS-patterned substrate could also present the dramatically improved hydrophilicity as compared to the APS ones. That is, ZnO nanoparticles in APS matrix could surprisingly promote the hydrophilicity of the testing microspots, which is of great importance for the applications of anchoring and analysis of biological molecules. Additionally, the ZnO-APS microspots could provide the functional amine groups necessarily for immobilizing the biological probes (i.e., antibodies) for the various applications of biological analysis (i.e., immunoassays). Therefore, the uniform and dense distributions of the testing

ZnO-APS microspots on the microarray would be expected for the better immobilization and throughput-improved detection of biomarkers with reproducible signal outputs.

Furthermore, the relationship between the hydrophobicity of the microarray substrates and the suppression of "coffee-ring" effects was investigated for controlling the distributions of ZnO-APS microspots on microarray. **Fig. 2** shows the photographic distributions of the ZnO-APS microspots on the HDS-patterned hydrophobic slides that were fabricated by using different HDS percents, with the hydrophobicities reflected by the contact angles. One can find that the "coffee-ring" effects could be gradually suppressed as the hydrophobicities of the HDS patterns increased. Again, the distribution uniformity of ZnO-APS microspots on the HDS

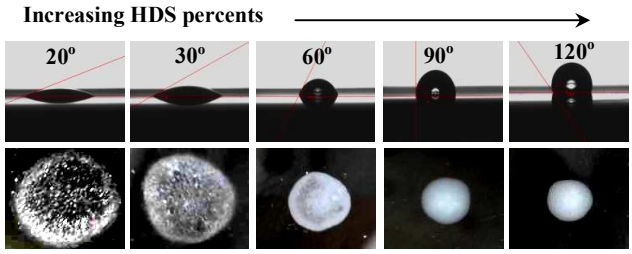


**Fig. 2** Photographic distributions of ZnO-APS microspots separately on the HDS-patterned hydrophobic slides constructed with different HDS percents (from left to right: 0.0, 0.10, 0.25, 1.0, 5.0 %) showing different contact angles.

patterns could depend on the hydrophobicity of the substrate surfaces. Subsequently, dense and uniform ZnO-APS microspots could be yielded as the contact angles went beyond 90°, which is thought to be resulted from the constraining force of hydrophobic HDS-patterned substrate during the solvent evaporation of the droplets, known as the Marangoni effects.[31] Therefore, the construction of hydrophobic substrates on the microarray could not only suppress the "coffee-ring" effects for the dense and uniform deposition of ZnO-APS microspots, but also provide a self-cleaning interface to minimize the crossing contamination of samples between the adjacent testing microspots on microarray. Hence, the throughput-improved fluorometric microarray analysis could be expected by using the developed HDS-ZnO-APS microarray with ZnO substrate-enhanced fluorescence.

The effects of the HDS percents and patterning time on the hydrophobicities of the microarray slides were further studied (**Fig. 3a**). It was discovered that the contact angles could increase as the increasing HDS percents. They could tend to be steady as the HDS percents increased over 5.0 %, 3.0 %, and 1.0 % as a function of patterning time of 2.0 h, 8.0 h, and 14.0 h, respectively. Accordingly, 5.0 % HDS and patterning time of 2 h were chosen to construct the desired hydrophobic HDS substrates in the whole experiments, if no special notice. Moreover, the APS percents used for the ZnO-APS microspots were optimized, with the ZnO dosage as a constant (**Fig. 3b**). Interestingly, the contact angles could decrease as the APS percents increased up to 0.30 %, over which they could tend to increase with a big increase in hydrophobicities. Herein, too high amounts of APS matrix might presumably increase the aqueous alkalinity resulting from the hydrolysis of amine-derivatized APS, so that the deposited ZnO nanoparticles would be etched to show the decreasing ZnO amounts,[32] leading to the decreasing hydrophilicities of ZnO-APS microspots on the hydrophobic HDS substrates. However, too low APS percents might challenge the deposition stability of the ZnO-APS microspots on microarray. Accordingly, APS percents of around 0.30 % - 1.0 % are suitable for depositing ZnO-APS microspots with the high hydrophilicities desirably for the biological tests.

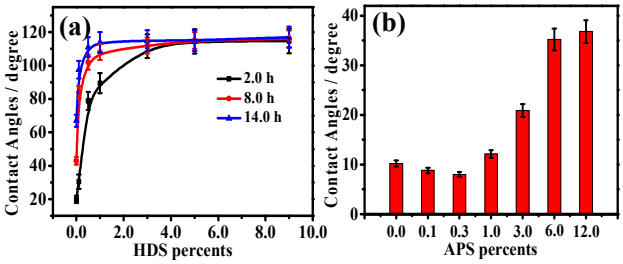


**Fig. 3** (**a**) HDS percents-dependent contact angles of HDS-patterned slides, which were fabricated as a function of patterning time (2.0 h, 8.0 h, and 14.0 h); (**b**) APS percents-dependent contact angles of HDS-ZnO-APS microarray slides, of which the ZnO-APS droplets with increasing APS percents were separately microspotted on the 5.0 % HDS patterns.

It was experimentally found that the APS percents could also influence the ZnO substrate-enhanced fluorescence of ZnO-APS microspots, including the shaping stabilities of sample droplets for the reproducible signal outputs. **Fig. 4a** exhibits the evidential photographs for the ZnO substrate-enhanced fluorescence of RB sample droplets under visible (up slide) and UV (down slide) light. Herein, different volumes of RB sample droplets (i.e., 1.0 μL, 2.0 μL, and 3.0 μL from up to down) were separately added on the ZnO-APS microspots created using various APS percents. As expected, the dramatically enhanced

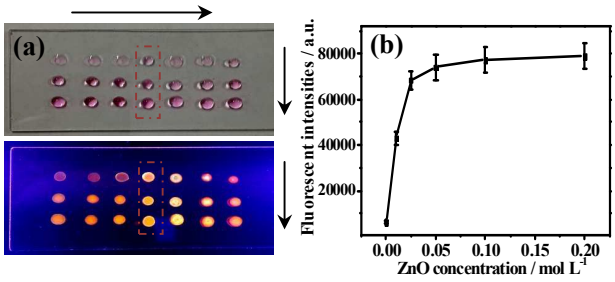


**Fig. 4** (**a**) ZnO substrate-enhanced fluorescence intensities on the ZnO-APS microspots created on HDS-patterned substrates using increasing APS percents (from left to right) indicated in **Fig. 3b**, characterized using different volumes of RB samples droplets (from up to down: 1.0, 2.0, 3.0 μL) under visible (up slide) and UV (down slide) light; (**b**) ZnO concentration-dependent fluorescence enhancement of RB sample droplets on the HDS-ZnO-APS microarray using different ZnO concentrations (insert: the photograph).

fluorescence of RB sample droplets were obtained on the surfaces of ZnO-APS microspots, in contrast to the APS deposited ones. Accordingly, the ZnO-APS microspots created

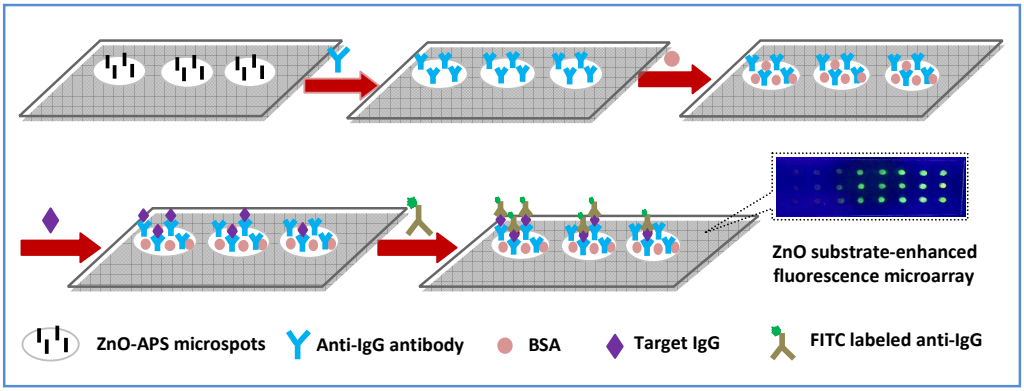


**Scheme 2** Schematic illustration of the detection protocol of the microarray-based sandwiched fluorescence immunoassays with ZnO substrate-enhanced fluorescence for IgG in human serum as a target model, of which the detailed detection procedure was shown in the Experimental.

with the APS percents of 1.0 % and 3.0 % could offer the relatively larger enhancement of fluorescent intensities of RB sample droplets. Moreover, the ZnO-APS testing microspots fabricated using the two APS percents could allow for the RB droplets deposited with no significant change of droplet shapes, despite different volumes of sample droplets were introduced. Here, it is thought that the hydrophobic substrates might exert favorably strong surface tension forces to restraint RB sample droplets within the testing areas of ZnO-APS microspots by balancing the gravity of the sample droplets, resulting in the well consistent shapes of sample droplets to promise the reproducible signal outputs. By compromising the optimal substrate-enabled fluorescence enhancement and the hydrophilicity for the modification of biological molecules above, 1.0 % APS was thereby selected for the fabrication of the ZnO-APS microspots on microarray. More importantly, ZnO concentration-dependent enhancement of RB fluorescence was observed (**Fig. 4b**), as shown in the corresponding photograph of RB sample droplets (insert). Accordingly, the fluorescence intensities of RB sample droplets on the ZnO-APS microspots could increase with the increasing ZnO concentrations till attaining the saturate at 0.050 mol $L^{-1}$, which was thus selected for the fabrication of the ZnO-APS microspots on microarray. Remarkably, the fluorescence intensities of RB sample droplets were about 10 fold larger on the ZnO-APS microspots than on the APS-coated ones without ZnO nanoparticles. The possible mechanism responsible for the fluorescence signals enhanced on the ZnO substrate might involve two pathways of the ZnO-triggered reduction of resonance energy transfer between the fluorophores themselves[33, 34] and the enhancement of evanescence wave and wave-guiding nature of the metal oxides for the fluorescent labels.[35-37] Moreover, the scanning electron microscope (SEM) imaging was conduct to explore the resulting ZnO-APS microspots (**Fig. 5a**). A uniform and dense distribution of ZnO-APS nanocomposites on the microarray, which served as the testing microspots, was observed, showing the average particle size of about 30 nm.

Under the optimized analysis conditions, the feasibility of the so developed microarray-based sandwiched fluorometry was investigated in probing immunoglobulin G (IgG) in human serum, as a model of biomarker for the clinical disease diagnosis. The sandwiched detection procedure is schematically illustrated in **Scheme 2**. Here, anti-IgG antibodies were covalently immobilized on the amine-derivatized ZnO-APS microspots on the microarray by glutaraldehyde cross-linking chemistry. Of note, the intrinsic fluorescence of ZnO nanoparticles could be quenched rapidly in the steps of the cross-linking treatment. After the blocking of any nonspecific protein binding sites, the immunoreactions could proceed after adding human IgG in serum to the anti-IgG-modified microspots. Furthermore, fluorescein isothiocyanate (FITC) labeled anti-IgG antibodies were introduced to recognize the captured IgG. **Fig. 5b** shows the dose-response curve for the microarray-based fluorescent detections of different IgG concentrations. It was found that the fluorometric analysis could present a rational change of fluorescence intensities enhanced by the ZnO substrates

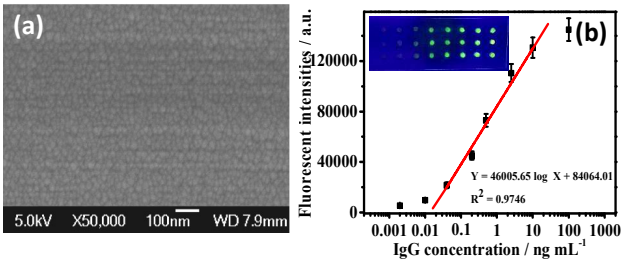


**Fig. 5** (**a**) Representative SEM image of the resulting surface of HDS-ZnO-APS microarray created using the optimum 1.0 % ZnO-APS droplets on 5.0 % HDS substrate; (**b**) the dose–response curve of the fluorometric sandwiched immunoassays with the HDS-ZnO-APS microarray for IgG in human serum, with the corresponding resultant image of fluorometric results (insert: each IgG concentration for tri-replicated tests).

depending on the IgG concentrations, as clearly demonstrated in the typical photograph of the microarray analysis results (**Fig. 5b**, inset). A linear relationship was achieved for the fluorescence intensities versus the IgG concentrations ranging from 0.010 to 10.0 ngmL$^{-1}$, with a limit of detection about 5.0 pg mL$^{-1}$ estimated by the 3σ rule. Therefore, the so developed functionalized microarray could allow for the throughput-improved and sensitive fluorometric analysis of biomarkers.

To summarize, functionalized fluorometric microarray was successfully fabricated by patterning the glass slides first with hydrophobic HDS and then microspotting with hydrophilic amine-derivatized ZnO-APS. The resulting HDS-ZnO-APS microarray could allow for the sandwiched fluorometric immunoassays with the substrate-enhanced fluorescence. On the one hand, the so fabricated hydrophobic HDS patterns could facilitate the highly dense and uniform distribution of ZnO-APS testing microspots on microarray by largely suppressing the "coffee-ring" effects to facilitate the throughput-improved fluorometric analysis. They could also functionalize the lotus-like "self-cleaning" to effectively minimize the crossing contamination of samples between the adjacent microspots and any interference of sample backgrounds, so that the simultaneous detections of multiple biomarkers in complicated media could be realized. On the other hand, the introduction of ZnO nanoparticles to work with the amine-derivatized APS could create the testing microspots with the greatly improved hydrophilicity for anchoring the meaningful biological probes. Especially, the ZnO substrate-enhanced fluorescence signals could be expected to achieve the high detection sensitivity of the microarray-based fluorometry. The feasibility of practical applications of the fluorometric microarray was demonstrated by the sandwiched immunoassays for IgG in serum samples, showing a detection limit down to about 5.0 pg $mL^{-1}$. It should be pointed out that the denser testing microspots would be created on microarray by a mechanical sample spotter to achieve even higher throughput of biomarker analysis. Importantly, the "dip and dry" fabrication procedure is simple and efficient for various functionalized fluorometric microarrays with ZnO substrate-enhanced fluorescence, without the need of any complicated light treatment or initiator. The developed microarray-based fluorometry may promise the potential applications for the analysis of multiple biomarkers of clinical importance.

This work is supported by the National Natural Science Foundations of China (No. 21375075 and 21573126), and the Taishan Scholar Foundation of Shandong Province, P. R. China.

## Notes and References

1. L. Yu, Y. Liu, Y. Gan and C. M. Li, *Biosens. Bioelectron.*, 2009, **24**, 2997-3002.
2. J. H. Rho and P. D. Lampe, *J. Proteome Res.*, 2013, **12**, 2311-2320.
3. J. H. Rho, J. R. Mead, W. S. Wright, D. E. Brenner, J. W. Stave, J. C. Gildersleeve and P. D. Lampe, *J. Proteomics*, 2014, **96**, 291-299.
4. M. I. Mohammed and M. P. Desmulliez, *Lab Chip*, 2011, **11**, 569-595.
5. X. Duan, L. Abuqayyas, L. Dai, J. P. Balthasar and J. Qu, *Anal. Chem.*, 2012, **84**, 4373-4382.
6. H. Zhu and M. Snyder, *Curr. Opin. Chem. Biol.*, 2001, **5**, 40-45.
7. B. D. Heij, C. Steinerta, H. Sandmaierb and R. Zengerlea, *Sensor. Actuat. A-Phys.*, 2003, **103**, 88-92.
8. S. Roy, J. H. Soh and Z. Gao, *Lab Chip*, 2011, **11**, 1886-1894.
9. F. L. Geyer, E. Ueda, U. Liebel, N. Grau and P. A. Levkin, *Angew. Chem. Int. Edit.*, 2011, **50**, 8424-8427.
10. S. Fujita, R. Onuki-Nagasaki, J. Fukuda, J. Enomoto, S. Yamaguchi and M. Miyake, *Lab Chip*, 2013, **13**, 77-80.
11.A.-E. Saliba, I. Vonkova, S. Ceschia, G. M. Findlay, K. Maeda, C. Tischer, S. Deghou, V. van Noort, P. Bork and T. Pawson, *Nat. Methods*, 2014, **11**, 47-50.
12. A. Szkola, K. Campbell, C. T. Elliott, R. Niessner and M. Seidel, *Anal. Chim. Acta*, 2013, **787**, 211-218.
13. J. Yan, S. Su, S. He, Y. He, B. Zhao, D. Wang, H. Zhang, Q. Huang, S. Song and C. Fan, *Anal. Chem.*, 2012, **84**, 9139-9145.
14.L. Hou, Y. Tang, M. Xu, Z. Gao and D. Tang, *Anal. Chem.*, 2014, **86**, 8352-8358.
15. B. Wu, C. Hu, X. Hu, H. Cao, C. Huang, H. Shen and N. Jia, *Biosens. Bioelectron.*, 2013, **50**, 300-304.
16. Y. Zhang, L. Ge, M. Li, M. Yan, S. Ge, J. Yu, X. Song and B. Cao, *Chem. Commun.*, 2014, **50**, 1417-1419.
17.G. C. Fan, L. Han, H. Zhu, J. R. Zhang and J. J. Zhu, *Anal. Chem.*, 2014, **86**, 12398-12405.
18. S. Xu, X. Ji, W. Xu, X. Li, L. Wang, Y. Bai, B. Zhao and Y. Ozaki, *Analyst*, 2004, **129**, 63-68.
19. W. Hu, Y. Liu, T. Chen, Y. Liu and C. M. Li, *Adv. Mater.*, 2015, **27**, 181-185.
20. A.-M. Alam, M. Kamruzzaman, S. H. Lee, Y. H. Kim, S. Y. Kim, G. M. Kim, H. J. Jo and S. H. Kim, *Microchim. Acta*, 2011, **176**, 153-161.
21. J. Zhang, A. Thurber, D. A. Tenne, J. W. Rasmussen, D. Wingett, C. Hanna and A. Punnoose, *Adv. Funct. Mater.*, 2010, **20**, 4358-4363.
22. W. Hu, Y. Liu, H. Yang, X. Zhou and C. M. Li, *Biosens. Bioelectron.*, 2011, **26**, 3683-3687.
23. N. Kumar, A. Dorfman and J. Hahm, *Nanotechnology*, 2006, **17**, 2875-2881.
24. Y. Zhang, H. Wang, J. Li, J. Nie, Y. Zhang, G. Shen and R. Yu, *Biosens. Bioelectron.*, 2011, **26**, 3272-3277.
25. G. McHale, *Analyst*, 2007, **132**, 192-195.
26. Y. Zhang, H. Wang, B. Yan, Y. Zhang, P. Yin, G. Shen and R. Yu, *J. Mater. Chem.*, 2008, **18**, 4442-4449.
27. R. D. Deegan, B. Olgica, T. F. Dupont , H. Greb, N. S. R. and W. T. A., *Nature*, 1997, **389**, 827-829.
28. D. S. Rickman, C. J. Herbert and L. P. Aggerbeck, *Nucleic Acids Res.*, 2003, **31**, e109.
29. J. M. Moran-Mirabal, C. P. Tan, R. N. Orth, E. O. Williams, H. G. Craighead and D. M. Lin, *Anal. Chem.*, 2007, **79**, 1109-1114.
30. J. M. Stauber, S. K. Wilson, B. R. Duffy and K. Sefiane, *Langmuir*, 2015, **31**, 3653-3660.
31. H. Hu and R. G. Larson, *J. Phys. Chem. B*, 2006, **110**, 7090-7094.
32. S. Li, Z. Sun, R. Li, M. Dong, L. Zhang, W. Qi, X. Zhang and H. Wang, *Sci. Rep.*, 2015, **5**, 8475.
33. A. Dorfman, N. Kumar and J. Hahm, *Adv. Mater.*, 2006, **18**, 2685-2690.
34.Y. Liu, W. Hu, Z. Lu and C. M. Li, *ACS Appl. Mater. Inter.*, 2014, **6**, 7728-7734.
35. V. Adalsteinsson, O. Parajuli, S. Kepics, A. Gupta, W. B. Reeves and J. Hahm, *Anal. Chem.*, 2008, **80**, 6594-6601.

36. M. Singh, S. Song and J. Hahm, *Nanoscale*, 2014, **6**, 308-315.
37. R. Kaiser, Y. Levy, N. Vansteenkiste, A. Aspect, W. Seifert, D. Leipold and J. Mlynek, *Opt. Commun.*, 1994, **104**, 234-240.